Leones, A.; Sonseca Olalla, A.; Lopez, D.; Fiori, S.; Peponi, L. (2019). Shape memory effect on electrospun PLA-based fibers tailoring their thermal response. European Polymer Journal. 117:217-226. https://doi.org/10.1016/j.eurpolymj.2019.05.014

Shape memory effect on electrospun PLA-based fibers tailoring their thermal-response.

Adrián Leonés[1], Agueda Sonseca[1], Daniel López[1], Stefano Fiori[2], Laura Peponi[1*]

1. Instituto de Ciencia y Tecnología de Polímeros, ICTP-CSIC, Calle Juan de la Cierva 3, 28006, Madrid, Spain
2. Condensia Química SA, R&D Department, C/ La Cierva 8, 08184 Barcelona, Spain

Abstract: A research on the thermally-activated shape memory behavior of electrospun nanofibers based on polylactic acid (PLA) plasticized with its oligomer (OLA) was conducted with the purpose of obtaining a suitable material to be used in potential biomedical applications. Three different PLA-OLA formulations with 70:30, 80:20 and 90:10 ratios were processed by electrospinning and studied in order to decrease the PLA glass transition temperature to a temperature closer to the human body. For each electrospun formulation mat, the average diameter of electrospun fibers was found to be 757±193nm for neat PLA and 768±207nm, 620±121nm and 476±80nm for PLA-OLA 90:10, 80:20 and 70:30 ratios, respectively and correlate it with their mechanical response. First of all, the PLA capability to present shape memory behavior even in non-woven electrospun fibers form has been studied at 60ºC. Thus, two values of switching temperatures (45°C and 40°C) were selected in order to evaluate their shape memory response, being temperatures close to the human body temperature. The recovery and fixity ratio of PLA-OLA formulations studied here showed suitable shape memory behavior of the electrospun systems with excellent values of strain fixity as well as strain recovery ratios indicating these materials appropriate for potential biomedical application.

Keywords: Electrospinning, polylactic acid, plasticizer, Shape Memory effect

Graphical Abstract:

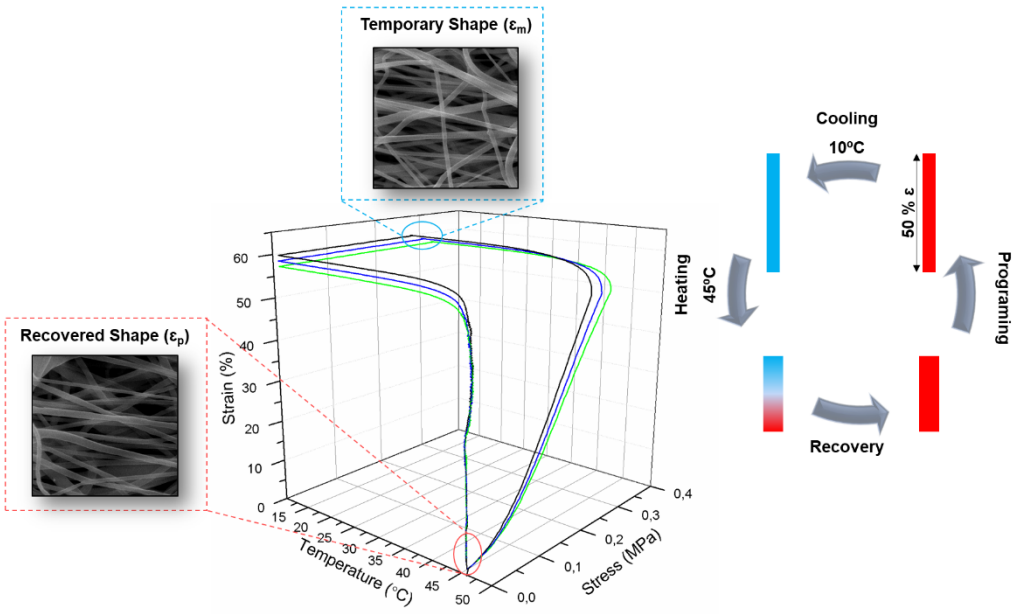

Highlights:

- PLA electrospun fibers showed thermally-activated shape memory response at 60ºC.
- The thermal response of electrospun PLA fibers has been tailored to temperature closer to the human body.
- Thermally-activated shape memory behavior is studied at 60ºC, 45ºC and 40ºC.
- Electrospun PLA plasticized materials showed an excellent capability of fixing a temporary form and recovering the original shape at 40ºC.

1. Introduction

Shape memory polymers (SMPs) are a class of smart materials able to recover their original shape from a previously temporary programmed shape when exposed to external stimuli of different nature (temperature, moisture, pH, light…)[1–5]. Therefore, the shape memory effect (SME) results from a combination of polymer chemistry, morphology and specific processing condition. These materials possess a tremendous potential in many fields as minimally invasive medical devices, actuators, sensors, smart textiles and so forth[6,7].

Depending on the structure of the materials, a classification into shape memory blocks, shape memory foams, shape memory fibers and shape memory films can be made[8,9]. Recently, SMPs with fibrous structure are gaining interest in applications that imply contact with the human body such as smart textiles or scaffolds for regenerative medicine[10]. In this sense, electrospinning process has been recognized as one of the most attractive technologies to produce fibrous structures[11,12], thanks to the advantageous high porosity and specific surface area obtained.

In recent years, polylactic acid (PLA) has been gaining interest for its use in the biomedical field as well as food packaging and textile thanks ~~to its wide variety of useful properties~~ [13–17]. Its non-petrochemical based nature, high tensile strength and elastic modulus, biocompatibility and degradability under physiological conditions into non-toxic products make PLA an ideal material for practical use in contact with the human body.

This versatile polymer is known to exhibit thermo-responsive shape memory effect[15,18–22], thanks to its glass transition temperature (T_g) acting as transition temperature, around 60°C. However, just considering potential biomedical application, its T_g is much higher than the human body temperature, together with its brittleness, poor toughness and elongation at break < 10%, limits its direct application. Thermally-activated shape memory in PLA is achieved by heating up to a switching temperature (T_{sw}) higher than T_g at which polymer chains have enough mobility to recover the original form from a temporary shape previously fixed. Thus, to consider the thermally-activated shape memory of PLA as a suitable way to change the temporary form of devices for biomedical application, a T_{sw} closer to the human body has to be achieved. Although numerous strategies based on copolymerization, blending or plasticization have been studied in order to modulate the final properties of PLA, only some blends, copolymers and nanocomposites were developed as bulk materials with shape memory

capability [4,15,20,23,24]. Example of poly(ester-urethanes) based on PLA are reporting in the literature, with a thermally-activated shape memory response at temperature closed to the human body [19].

However, examples of electrospun fiber mats have been used also in order to obtain composite materials in form of bilayers or multilayers [25,26]. Zhang et al. [27] reported an example of electrospun PLA-based composite with shape memory effect as well as by Luo et al. [28]

With this background, in this work, we investigated plasticization as a practical and economic way to decrease the glass transition temperature of PLA-based electrospun materials. Several additives to reduce the T_g of PLA have been studied[29–34], but their compatibility and miscibility with PLA is limited. At this regards, the use of oligomers of lactic acid (OLA) could be an alternative to get plasticizers with high compatibility with PLA due to their similar chemical structure[30]. Additionally, it is well known that PLA is degraded into monomeric and oligomeric lactic acid inside the body, both products tested as safe and able to be secreted from the body. Therefore the use of OLA as plasticizer might not limit the biomedical applications of PLA[14]. A preliminary study reported in the literature of OLA with different molecular weights acting as PLA plasticizer at 15wt% showed a significant decrease in T_g to a range of 36-40ºC and an improvement in elongation up to 200% while good mechanical properties were still retained [35]. Therefore, in the present work, a commercial oligomer based on $_{D,L}$-lactic acid have been tested as a promising additive in order to modulate the T_g of PLA and achieve a good thermo-responsive shape memory performance of non-woven electrospun PLA mats at a temperature close to the human body. First of all, to the best of our knowledge, this is the first time in which thermally-activated shape memory behavior has been studied on PLA electrospun fibers at 60ºC. Moreover, in order to tune the thermally-activated shape memory response of PLA, PLA-OLA systems were studied to achieve shape memory electrospun fibers suitable for further applications in the human body. Thus, different electrospun fiber mats of PLA with its oligomer acting as plasticizer were processed and characterized. In particular, their thermo-mechanical cyclic shape memory behavior was studied at three different temperatures (60ºC, 45°C and 40°C) and their shape memory performance was discussed through the capability to fix the temporary shape as well as to recover its original one.

2. Experimental

2.1 Materials

Polylactic acid (PLA3051D, 3% of D-lactic acid monomer, molecular weight 142 × 10^4g.mol^{-1}, density 1.24g.cm^{-3}) was supplied by NatureWorks®. Lactic acid oligomer (Glyplast OLA8, ester content >99%, density 1.11g.cm^{-3}, viscosity 22.5mPa.s, molecular weight 1100g.mol^{-1}) was kindly supplied by Condensia Quimica SA. Chloroform ($CHCl_3$) (99.6% purity) and N,N-dimethylformamide (DMF) (99.5% purity) from Sigma Aldrich were used as solvents.

2.2 Processing of electrospun PLA-OLA samples

PLA pellets were dried in oven overnight at 60°C previous to use. Table 1 shows the different proportions of polymer and plasticizer used with a final concentration of 10wt% in $CHCl_3$:DMF (4:1) [36]. Each solution was stirred overnight at room temperature before the electrospinning process as indicating in our previous work of protocol optimization [29,36,37] .

Table 1: PLA and PLA-OLA formulations.

Sample	PLA (wt%)	OLA (wt%)
PLA	10	0
PLA90	90	10
PLA80	80	20
PLA70	70	30

Electrospun fiber mats were prepared in an Electrospinner Y-flow 2.2.D-XXX (Nanotechnology Solutions) in vertical configuration coupled to coaxial concentric needles. Polymer solutions were pumped through the inner needle and a $CHCl_3$:DMF (4:1) solvent solution was pumped through the outer needle. An electric field of 10kV in positive and -10kV in negative pole were set. The solvent solution and polymer solution flow rates were fixed at 0.50mL.h^{-1} and 3.5mL.h^{-1}, respectively. Each formulation was electrospun for 3h over a metal plane collector covered with aluminum foil placed at 14cm distance from the needle. The obtained mats were vacuum dried for 24h in order to remove any solvent residues.

2.3 Characterization techniques

Scanning Electron Microscopy, SEM, (PHILIPS XL30 Scanning Electron Microscope) was used in order to study the morphology of the electrospun fibers. All the samples were previously gold-coated (~5nm thickness) in a Polaron SC7640 Auto/Manual Sputter. SEM images analysis were carried out with ImageJ software. Diameters were calculated as the average value of 30 random measurements for each sample.

Thermal transitions were studied by Differential Scanning Calorimetry in a DSC Q2000 TA instrument under nitrogen atmosphere (50mL.min^{-1}). The thermal analysis was programmed at 10°C.min^{-1}from -60°C up to 180°C obtaining the glass transition temperature (T_g) calculated as the midpoint of the transition, , the melting temperature (T_m), the cold crystallization enthalpy (ΔH_{cc}) and the melting enthalpy (ΔH_m). The degree of crystallinity (X_c%) was calculated using the equation 1, taking the value of crystallization enthalpy of pure crystalline PLA (ΔH_m^0) as 93.6J.g^{-1} and W_f as the weight fraction of PLA in the sample[38].

$$X_c\% = 100 \times \left(\frac{\Delta H_m - \Delta H_{cc}}{\Delta H_m^{0\,\circ}}\right) \times \frac{1}{Wf} \qquad \text{Equation 1}$$

Mechanical properties were evaluated by tensile test in a QTest™ 1/L Elite instrument equipped with a 100N load cell at room temperature. Strain rate and initial length between clamps were set at 10mm.min^{-1} and 10mm respectively. Samples of 10mm length, 6mm width and 100µm of average thickness were measured and results from five specimens were averaged. Young Modulus (obtained as the slope of the curve from 0% to 2% deformation) and maximum stress and elongation at break were calculated.

Dynamic Mechanical Thermal Analysis (DMTA) was carried out in a DMA Q800 TA instrument working with clamp tension mode. An amplitude of 10µm, a frequency of 1Hz and a heating rate of 2°C.min^{-1} were used. In addition, thermally-activated shape memory properties were quantified by thermo-mechanical cyclic tests. The instrument was set in controlled force mode and four different stages were defined for each cycle: (1) The sample was equilibrated at the chosen switching temperature (T_{sw}) for 5min (three different temperatures were studied such as 60°C, 45ºC and 40°C) and then, a ramp stress of 0.2MPa.min^{-1} was applied until the sample reached 50% of deformation. (2) The sample was subsequently cooled at a fixing temperature (T_{fix}) of 10°C under constant stress in order to fix the temporary shape. (3) After releasing the stress at 0.50MPa.min^{-1}, the sample was heated at 3°C.min^{-1} up to T_{sw} and maintained for 30min

in order to recover the initial permanent shape. Sample dimensions for the DMTA and shape memory tests were the same as for the previously described mechanical tests.
The quantification of the shape memory behavior was carried out by calculating the strain fixity ratio (R_f) and the strain recovery ratio (R_r) given by equations 2 and 3[19]:

$$R_f(N) = 100 \times \frac{\varepsilon_u(N)}{\varepsilon_m(N)} \quad \text{Equation 2}$$

$$R_r(N) = 100 \times \frac{\varepsilon_m(N) - \varepsilon_p(N)}{\varepsilon_m(N) - \varepsilon_p(N-1)} \quad \text{Equation 3}$$

Where ε_m is the maximum strain after cooling to T_{fix} and before releasing the stress, ε_u is the fixed strain after releasing the stress at T_{fix} and ε_p is the residual strain after retaining the sample at T_{sw} for 30 minutes. As was pointed before, three different T_{sw} temperatures were tested which were selected taking into account the DSC results and in order to proof the capability of the samples to be useful for future biomedical applications.

3. Results and discussion.

First of all, once obtained the different electrospun mats, their fiber morphologies were studied by Scanning Electron Microscopy of each sample. SEM images for neat PLA and PLA-OLA system with ratios 90:10, 80:20 and 70:30 are shown in Fig.1. As it can be seen, straight, randomly oriented and bead-free fibers were obtained with an average diameter of 757±193nm for neat PLA and 768±207nm, 620±121nm and 476±80nm for PLA-OLA 90:10, 80:20 and 70:30 ratios, respectively. SEM images of electrospun mats at low magnifications and the corresponding diameter distribution of the electrospun fiber mats are reported in Supporting Information as Figure SI1. As expected, fiber diameter decreases with the addition of plasticizer due to the interaction between PLA and OLA[27,34]. The morphology of the fibers reveals the correct electrospinning process carried out for each sample despite showing some beads in the solution with the highest OLA concentration.

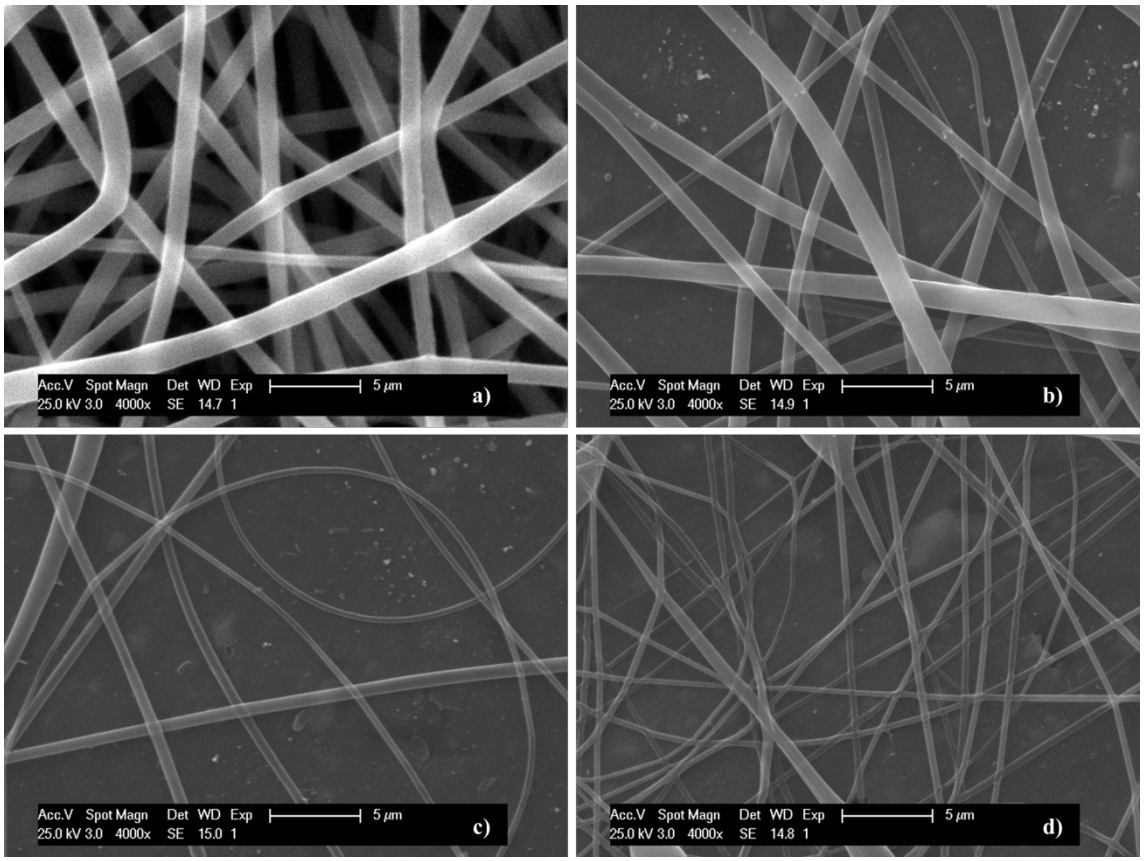

Fig. 1: SEM images of electrospun mats from: a) PLA 10wt%, b) PLA-OLA (90:10), c) PLA-OLA (80:20) and d) PLA-OLA (70:30).

The thermal and mechanical characterization was carried out with the aim of setting the parameters for the further shape memory analysis.

In Figure 2, the DSC thermograms are reported for all the samples studied. The arrow indicates the Tg shift towards less values by increasing the amount of OLA in the electrospun mats.

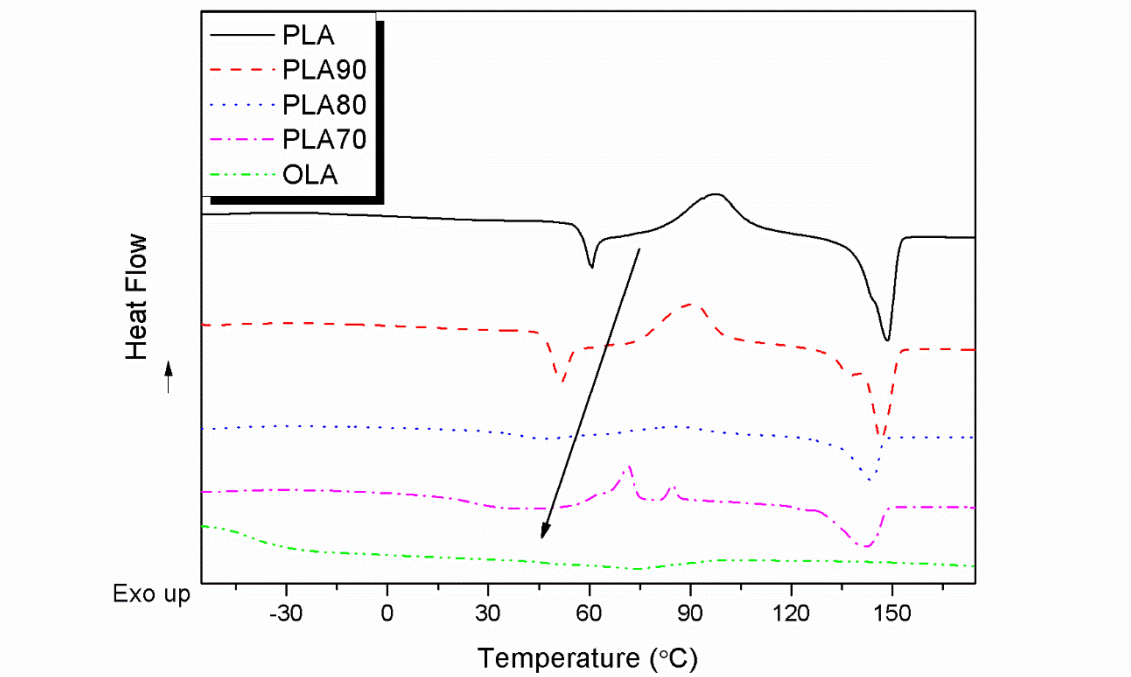

Fig. 2: DSC thermograms for the different electrospun mats formulation.

Table 2 summarizes the results obtained for each non-woven electrospun mat of the different PLA-OLA formulations.

Table 2: Thermal behavior of PLA-based mats.

Sample	DSC						
	W_{PLA}	T_g (°C)	ΔH_{cc} (J/g)	T_{cc} (°C)	T_m (°C)	ΔH_m (J/g)	X_c (%)
PLA	1.0	60	27.8	99	149	32.7	5
PLA90	0.9	47	29.0	91	147	29.9	1
PLA80	0.8	35	24.0	90	144	24.1	1
PLA70	0.7	21	22.4	71/84	142	25.5	5
OLA		-43			73	10.5	11

The similar values of the cold-crystallization enthalpy and the melting enthalpy for the neat PLA mat and plasticized PLA-OLA systems indicates that samples were quite amorphous.

However, it is important to point out that , in general, the crystallinity of electrospun polymers can often be significantly different to bulk materials. So, in Supporting Information file we provide the DSC traces for PLA/OLA films obtained by solvent casting, as new Figure SI2. Moreover, the degree of crystallinity has been calculated also for the bulk formulations, and summarized in the inset of Figure SI2. In this case, the degree of crystallinity is very different comparing the materials obtained as

electrospun-mats or as film for solvent casting, indicating that the processing conditions as well as the processing itself deeply affect the final properties of the materials.

Moreover, is important to focus that the glass transition temperature is shifted to lower temperatures with increasing the amount of OLA due to the plasticizing effect in which the addition of 30wt% of OLA results in T_g of 21ºC. However, a T_g slightly closer to body temperature occurs for the sample with a 20wt% of OLA indicating a better control of the shape memory behavior at a temperature closer to the human body. Thus, from the overall DSC results is emerged that it is possible to trigger the T_{sw} value by changing the amount of plasticizer.

From the mechanical point of view, Young´s Modulus, elongation at break and maximum stress values of PLA-OLA and neat PLA electrospun mats derived from the tensile stress-strain test (Fig.2), are summarized in Table 3.

Table 3: Tensile properties of PLA-OLA samples.

Sample	Young´s Modulus (MPa)	Max. stress (MPa)	ε break (%)
PLA	91±8	3.8±2	135±10
PLA90	63±14	3.6±1	125±9
PLA80	64±6	2.5±1	140±27
PLA70	30±16	2.1±1	146±30

Neat PLA electrospun fibers mat is characterized by the highest Young´s modulus (91±8MPa) and tensile strength (3.8±2MPa) being on the range of those reported on the literature for random electrospun mats (Young´s Modulus ~90MPa; Max. Stress ~3MPa)[16]. Addition of 10 and 20wt% of OLA (PLA-OLA 90:10 and PLA-OLA 80:20) lowers the Young´s Modulus to 63-64MPa, although is still higher than that obtained for PLA-OLA 70:30 (30±16MPa). The addition of 10wt% of plasticizer allows retaining almost the same value of the tensile strength that neat PLA (3.6±1MPa) while higher contents (20-30wt% of OLA) shifted it towards lower values. In general, the higher toughness, the lower T_g, and the lower Young´s modulus while the tensile strength is retained, is advantageous from the medical application point of view for imparting greater flexibility making PLA materials suitable for soft tissue engineering, wound healing or smart textiles applications. In our case, the mechanical properties of PLA-OLA mats are comparable with the Young´s modulus of human tissues i.e. human articular cartilage (10-21MPa) and skin (3-54MPa), and therefore comparable with

other PLA-based electrospun fibrous scaffolds for soft tissue engineering (Young´s Modulus 57.38±0.81MPa; Max. Stress 3.57±0.81MPa) [39–42].

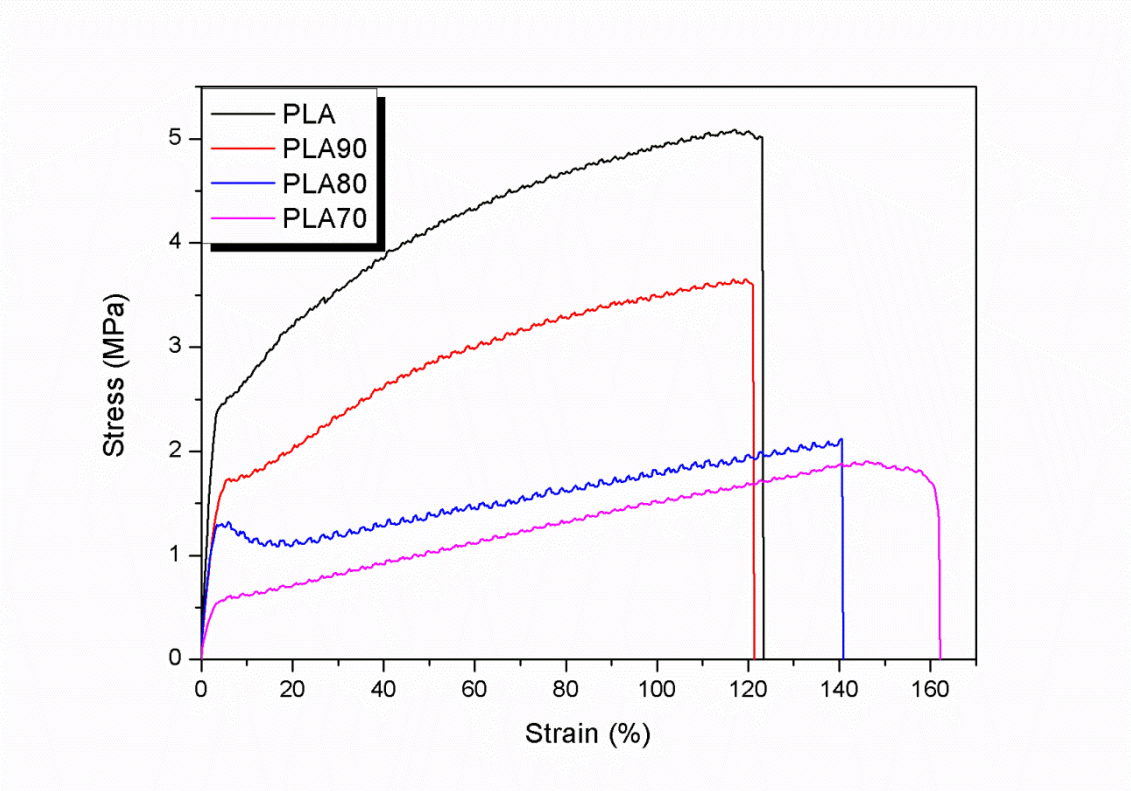

Fig. 3: Tensile stress-strain test for the electrospun mats.

The study of the main thermo-mechanical relaxations through DMTA of PLA-OLA samples give an important information in order to further perform and understand the shape memory performance. The evolution of the storage modulus (E´) and loss modulus (E´´) as a function of temperature are presented in Figure 4.

The addition of OLA seems to increase the storage modulus of the system at low temperature (-50 to 20ºC). We retain that this phenomenon can be attributed to the crystalline nature of OLA. In fact, the OLA presents a very broad melting peak (see figure 2), from 20 to 100ºC with a melting temperature of about 70ºC, indicating that at temperature below 20 ºC the OLA is crystalline.

The peak of loss modulus (E´´) is clearly shifting to lower temperatures and broadening in width with the increase of the OLA content. The movement of the peak towards lower temperatures is related with the energy required to activate the molecular mobility, being lower (molecular mobility easily activated) for PLA-OLA samples than for neat PLA in agreement with the DSC results, where Tg values of the electrospun mats contain OLA shift towards less temperatures respect to PLA electrospun fibers.

The sample PLA70, with the highest content of OLA, shows 2 different Tg. The first one related to the OLA-rich phase and the second one related to the PLA-rich phase in the system. In the DSC it is also possible to detect a very small Tg at about -15 ºC and another one, more pronounced, at 21ºC, related to the PLA-rich phase. This fact can only be detected in the system with the highest content of OLA, where it is possible that a phase separation occurs obtaining two different phases, one more rich in OLA and a second one more rich in PLA.

Moreover, from the DMA analysis, a clear increase in mechanics above the Tg, which could be the result of cold crystallization, can be detected in agreement with the DSC results.

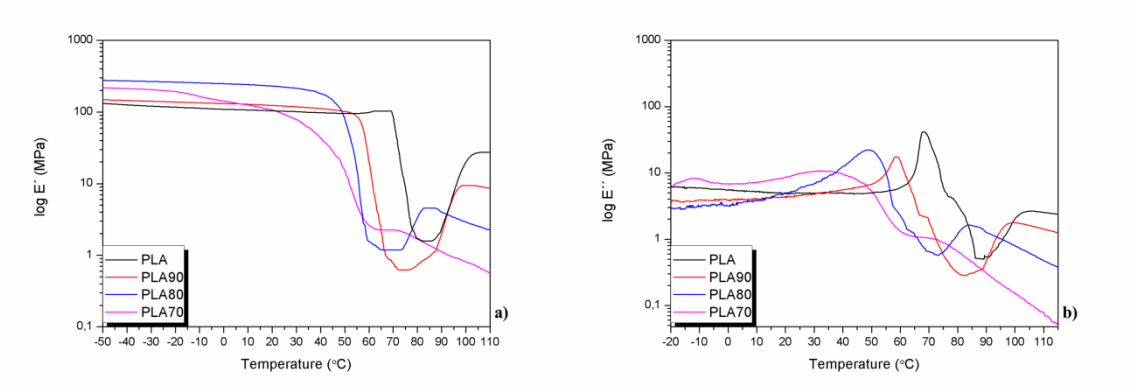

Fig. 4: Dynamical mechanical thermal analysis for each mat formulation.

Therefore, thus considering the shift of the T_g from 60ºC to lower values by increasing the OLA amount, three different temperatures (T_{sw} = 60ºC, 45°C and 40ºC) were used for neat electrospun PLA and plasticized samples (PLA-OLA) in order to quantify their shape memory behavior. These temperatures are in good agreement for materials with further potential application in biomedicine.

First of all, taking into account that there are no previous reports about the shape memory capacity of non-woven PLA fiber mats processed by electrospinning, its shape memory behavior was studied at 60°C.

Figure 5 shows the shape memory cyclic behavior of neat PLA electrospun fibers demonstrating the capability to completely fix the temporary form and recover its original shape at 60°C. As can be seen in Table 4 the material shows a recovery ratio (R_r) higher than 95% in all cycles and a fixity ratio (R_f) ~ 90% similar to the values reported for film samples (R_r ~75% and R_f ~98%) [43] indicating the excellent shape memory response of non-woven electrospun PLA fiber mats.

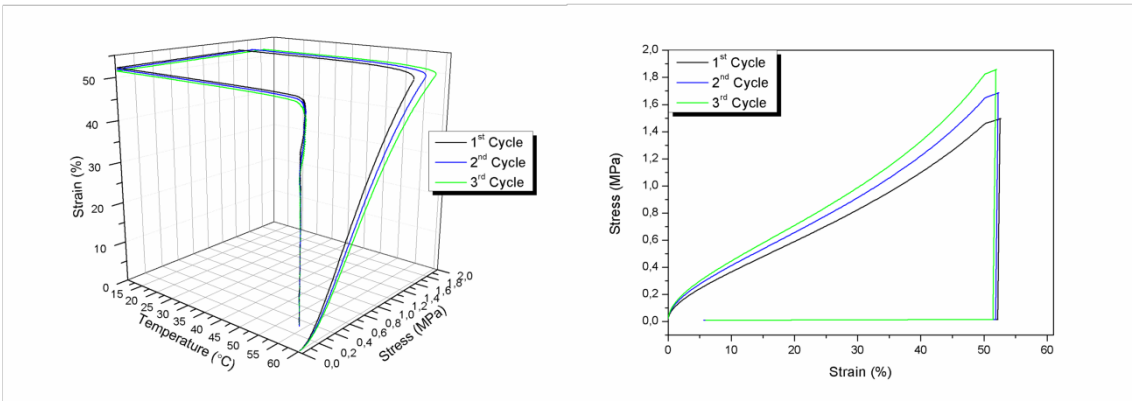

Fig. 5: 3D and 2D thermo-mechanical cycles performed at 60°C for neat electrospun PLA fibers.

Once verified that electrospun PLA mats show excellent shape memory behavior, we study the shape memory response of the plasticized systems. ~~Every~~ Plasticized systems have been studied at 60ºC and 2D and 3D shape memory thermo-mechanical cycles for the plasticized systems are reported in figure 6.

It is easy to note that all the materials are able to fix their temporary shape and to recover their original one presenting shape memory behavior with good values for R_f and R_r (table 4). However, taking into account that the plasticized systems present lower T_g than PLA, it is easy to point out that the temperature needed for the activation of the shape memory response is lower than 60ºC. In particular, PLA-OLA 90:10 needs a temperature of 50ºC, PLA-OLA 80:20 needs a temperature of 35ºC and PLA-OLA 70:30 needs a temperature of 20ºC to start their recovery. These temperatures are in completely agree with their T_g values. For this reason, we choose to study the thermally-activated shape memory response of the plasticized materials at 45ºC and 40ºC, considering also their potential application for devices in contact with the human body.

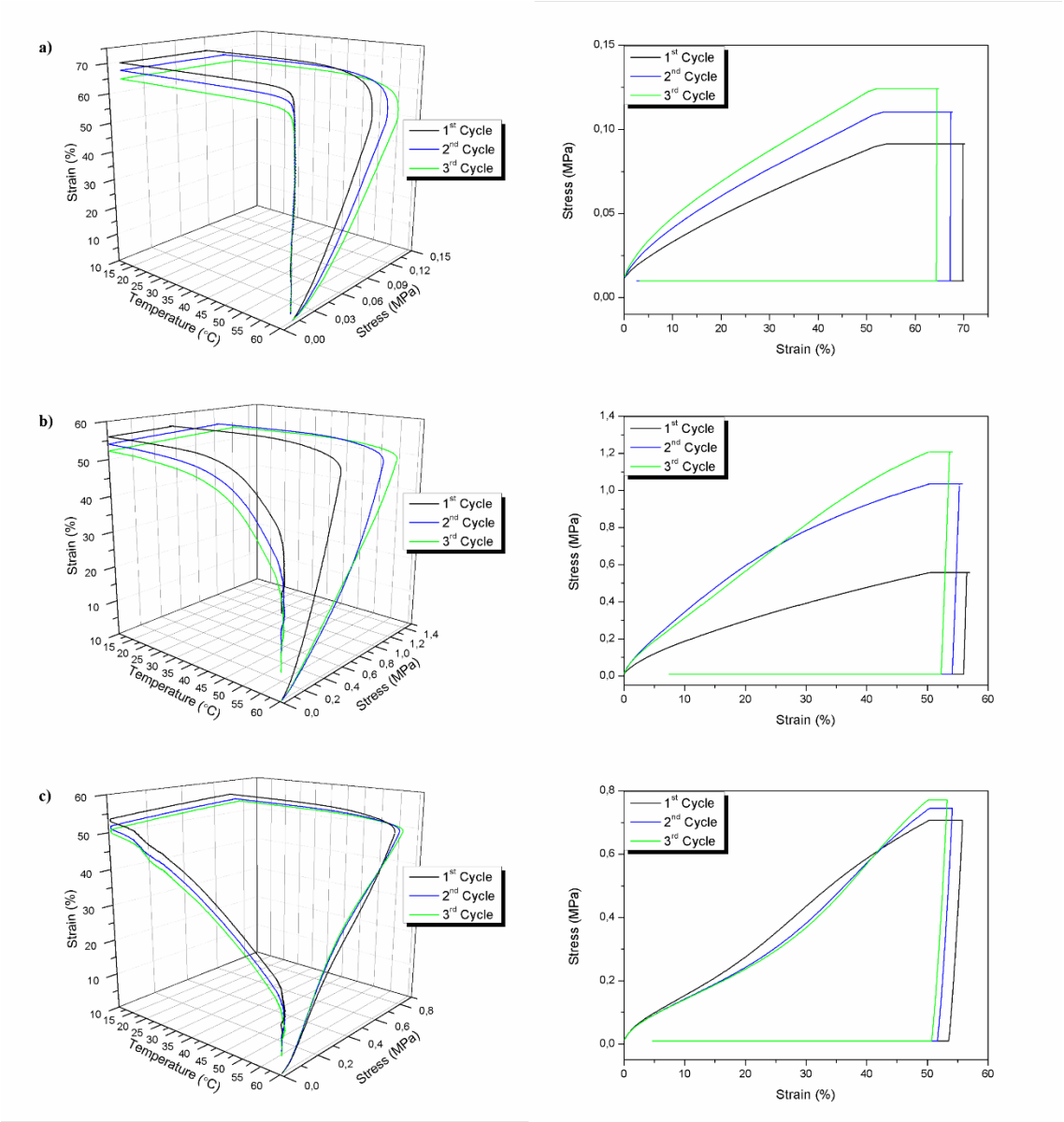

Fig. 6: 3D and 2D thermo-mechanical cycles performed at 60°C for a) PLA-OLA 90:10, b) PLA-OLA 80:20 and c) PLA-OLA 70:30.

Moreover, 2D and 3D thermo-mechanical cycles for the first cycle of all the samples studied at 60ºC are reported as Figure SI3, in the supporting information, in order to easily visualize as the addition of plasticizer influences the PLA response.

Figure 7 and figure 8 show the thermally-activated shape memory cycles for PLA-OLA 80:20 and PLA-OLA 70:30, respectively, at 45ºC and 40ºC, thus taking into account that, as we expect, both neat PLA and PLA-OLA 90:10 do not show shape memory behavior at these temperature being lower than their T_g (figures not shown).

As can be seen in Table 4 and Fig. 7, PLA-OLA 80:20 sample showed excellent capability to fix the temporary shape at 45°C, with R_f values of 100% for the first

thermo-mechanical cycle maintaing quite constant in the other cycles with values higher than 95%. Additionally, a R_r of 100% was achieved showing an excellent shape recovery of the original shape at 45ºC during all the thermo-mechanical cycles. At 40ºC the capability of the material to fix the temporary shape is maintained with R_f of 98% in all the cycles. However, a slightly low R_r indicates a low capacity to recover the original shape at 40ºC, due to the small variation of only 5ºC with its T_g.

On the contrary, PLA-OLA 70:30 show better thermally-activated shape memory response at 40ºC than 45ºC. In fact, samples with 30wt% of OLA broke during the third cycle in the performed thermo-mechanical shape memory tests at 45ºC, showing an optimal capability to fix the temporary shape with R_f values higher than 90% in the first two cycles and a quite good capability of recovery the original shape with R_r in the range of 70%. However, at 40ºC the ability of the material to both fix the temporary shape and recover the original shape are maintaining constant during all the thermo-mechanical cycles with values of 92% and 75%, respectively. Hoverer, it is worth to note that at a temperature higher than 20ºC the sample starts to recovery their original shape. These results are strongly correlated with the T_g of the materials, in the last case much lower than 40ºC.

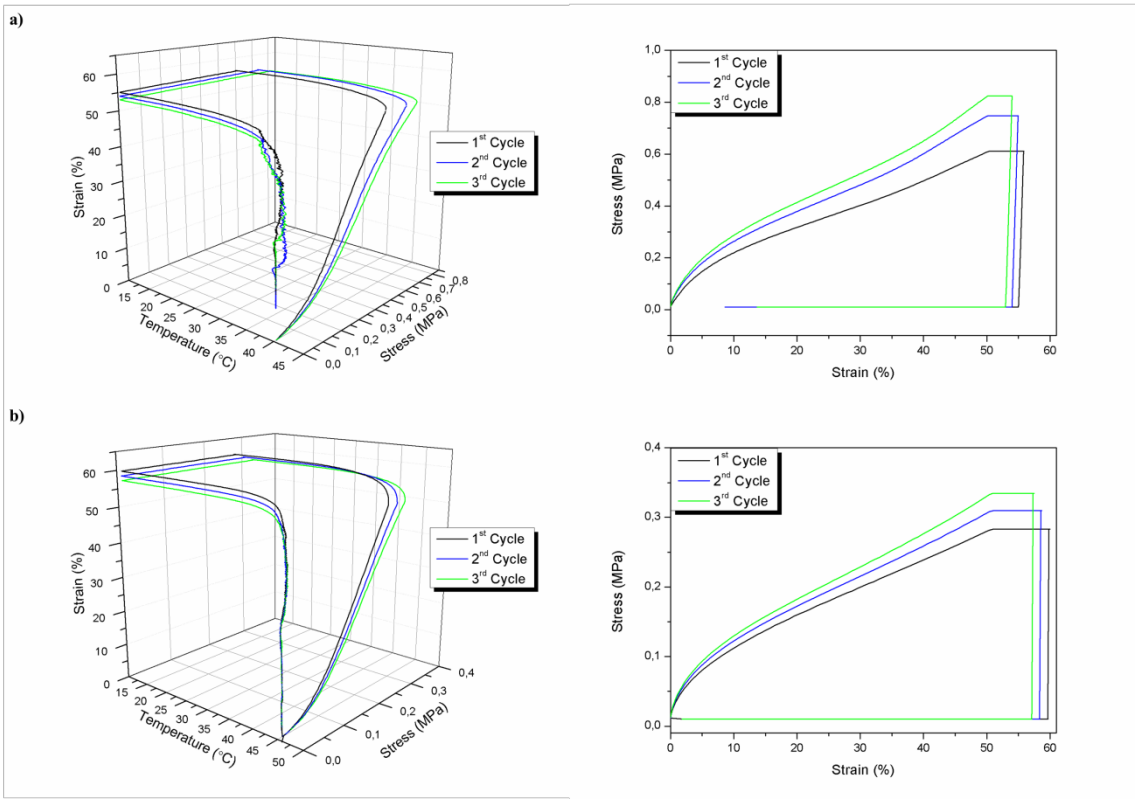

Fig. 7: 3D and 2D thermo-mechanical shape-memory cycles performed at: a) 40°C and b) 45°C for PLA-OLA 80:20 electrospun sample.

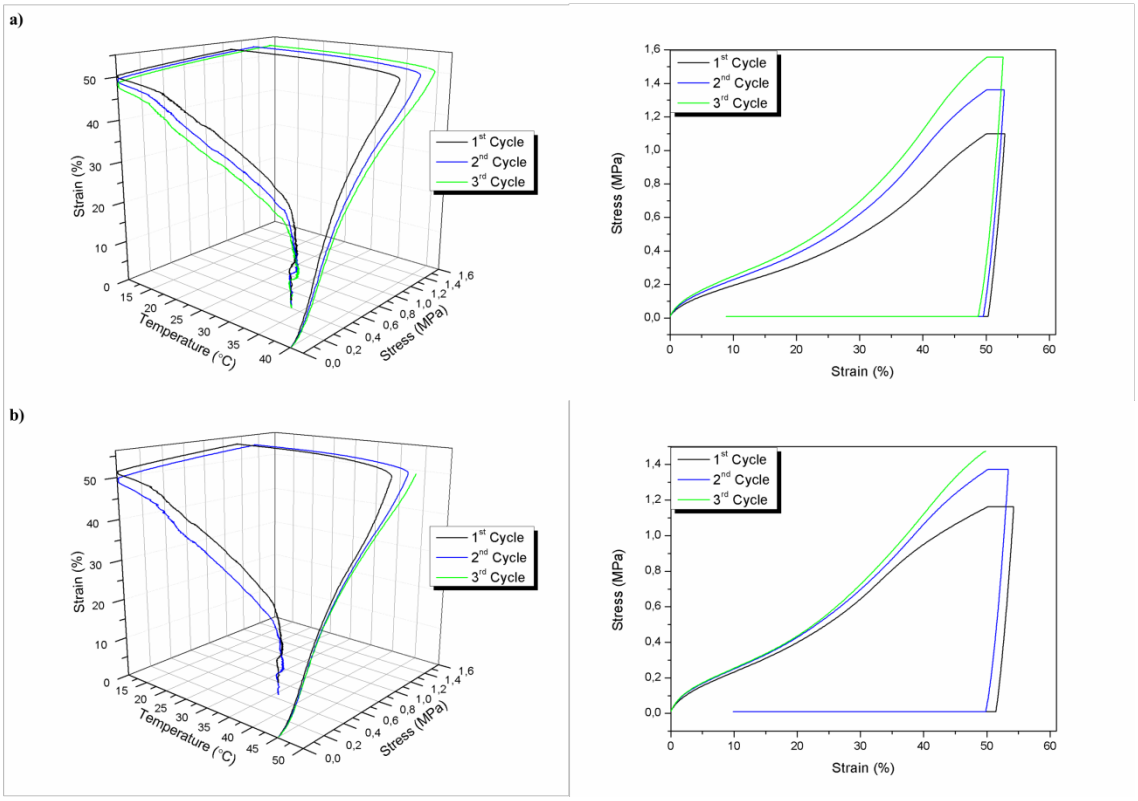

Fig. 8: 3D and 2D thermo-mechanical cycles performed at: a) 40°C and b) 45°C for PLA-OLA 70:30 electrospun sample.

Table 4: Values of strain recovery ratio and strain fixity ratio at different temperatures.

Sample	R_r (%)			R_f (%)			T_{sw} (C°)
	1st cycle	2nd cycle	3rd cycle	1st cycle	2nd cycle	3rd cycle	
PLA	89	88	88	96	99	99	60
PLA90	96	72	73	74	76	78	60
PLA80	61	71	82	90	93	96	60
PLA70	84	88	91	95	99	100	60
PLA	--	--	--	--	--	--	45
PLA90	--	--	--	--	--	--	45
PLA80	100	100	100	100	97	95	45
PLA70	71	73	--	94	92	--	45
PLA	--	--	--	--	--	--	40
PLA90	--	--	--	--	--	--	40
PLA80	86	91	79	98	98	98	40
PLA70	74	75	75	94	92	92	40

Therefore, taking into account the shape memory results of neat and plasticized non-woven electrospun PLA mats, PLA-OLA with 20wt% of plasticizer ideally represents the best material for future biomedical applications due to the fact that it shows excellent shape fixity and shape recovery capability at temperature close to the human

body activating shape changes without applying temperatures harmful for surrounding tissues.

In order to compare the different behavior of unplasticized and plasticized PLA, in Figure 9, 2D strain-time graph has been reported for PLA at 60ºC and PLA80 at 60, 45 and 40ºC, evidencing the different stage of the thermo-mechanical cycle used to study the shape memory behavior. A first deformation is followed by the fixity of the temporary shape and then, heating again the materials, the recovery of the original shape occurred. In particular, it is easy to note that all the sample show excellent fixity behavior. The recovery time is affected by the temperature as well as by the use of plasticizer. In particular, for PLA at 60ºC a time around of 30min is necessary to recover the original shape. The same 30min are necessary for PLA80 at both 40 and 45ºC, while for PLA80 at 60ºC about 20min are enough to recover its original shape. We can correlate this phenomenon with the values of their Tg, being the recovery time as bigger as the temperature used is closer to the Tg.

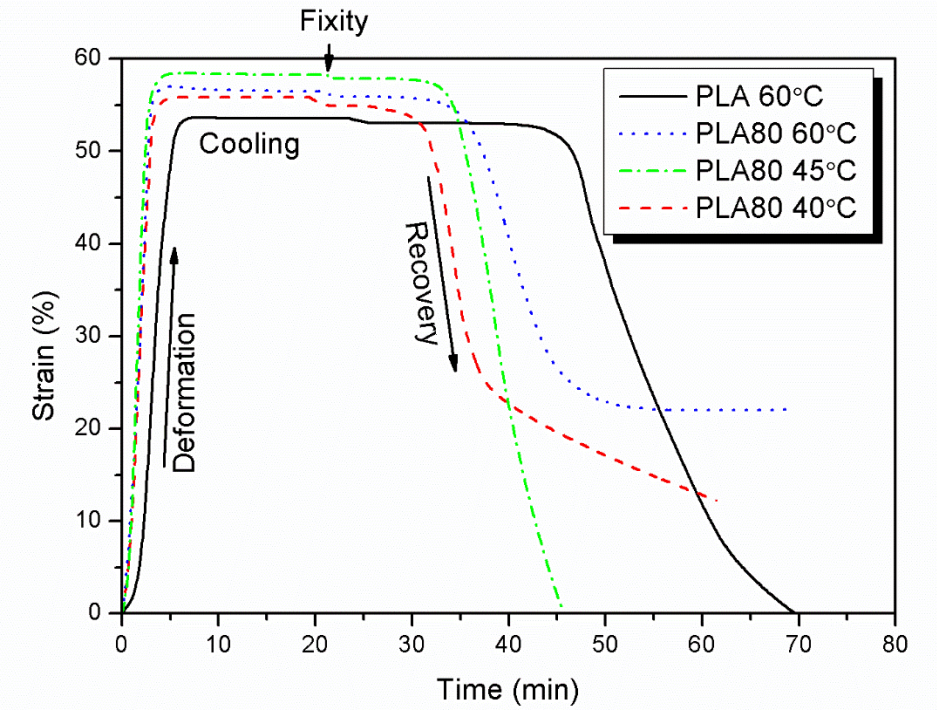

Fig. 9: 2D strain-time diagram for PLA at 60ºC and PLA80 at the three different temperatures studied.

Finally, the thermally-activated shape memory effect of non-woven electrospun plasticized PLA-OLA materials was proved macroscopically (Figure 10). Temporary shape was programmed by deforming the sample at 45ºC and cooling down in order to fix the temporary shape and then the recovery of the permanent shape was driven by heating again the sample at 45ºC. Pictures were taking at different recovery times in order to visualize its effect. In particular, for PLA-OLA 80:20, our best formulation, 10 seconds are enough to recover the initial shape of the electrospun fibers at 45ºC indicating a very fast shape memory phenomenon.

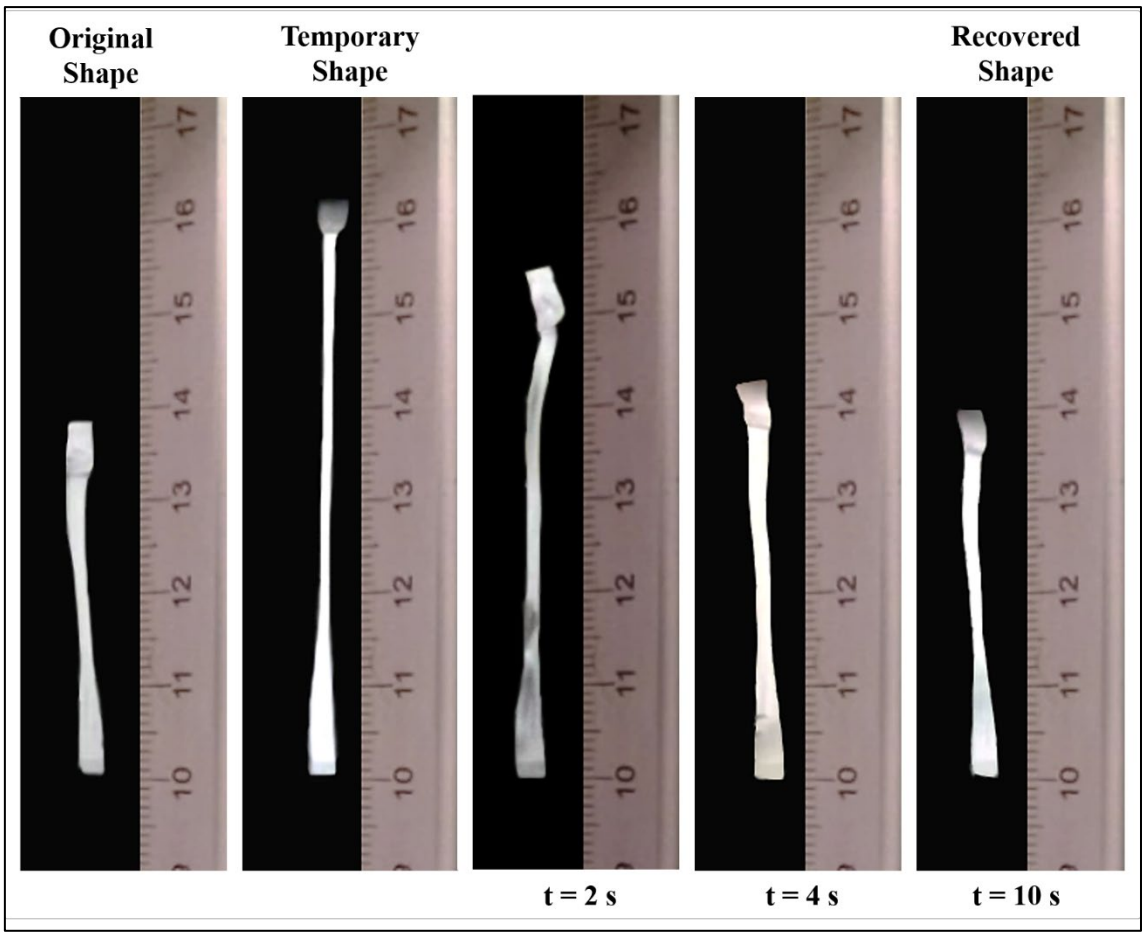

Fig. 10: Macroscopic demonstration of the shape memory effect for electrospun PLA-OLA 80:20 sample at 45ºC.

Interesting is also to study the microstructural changes on the structure of the fiber mats during the thermo-mechanical shape memory cycles, shown in Figure 11. The original sample shows a randomly oriented distribution of fibers. When temporary shape is programmed, the fibers seem to be oriented in the direction of the applied stress,

representing by arrows in the figure 9. A slightly decrease of the diameter (473±115nm) is showed in comparison with the diameter of the original sample (620±121nm). Finally, when original shape is recovered, the fibers maintain the induced orientation applied during the programming stage but increasing the diameter of fibers up to 817±104nm.

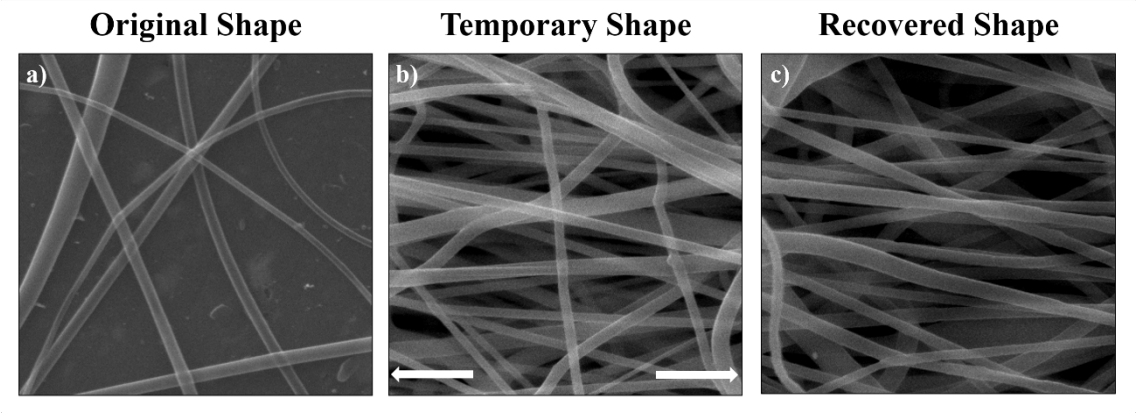

Fig. 11: SEM images of the shape memory effect for electrospun PLA-OLA 80:20 sample at 45ºC: a) original shape, b) temporary shape and c) recovered shape.

4. Conclusions

In this work, shape memory PLA-based electrospun mats with thermally induced effect in the range of interest for potential biomedical applications were successfully prepared by incorporating different amounts of polylactic acid oligomer (OLA) with the electrospinning process. It was observed a random orientation in all the samples as well as a clear influence of the amount of OLA over the morphology and diameters of the obtained fibers. As the amount of OLA into the samples increased, fiber morphology changed from uniform to irregular fibers with some beads and the fiber diameter decreased from 757±193nm for neat PLA to 476±80nm for PLA-OLA with the highest amount of OLA, 30wt%. Furthermore, the addition of OLA promoted a decrease in the glass transition temperature from 60ºC for neat PLA towards a range closer to the physiological temperature (47-21ºC) and allowed to tailor the mechanical behavior of the mats to be more similar to that of the living tissues. Therefore, three different temperatures of 60ºC, 45ºC and 40ºC were used to evaluate the thermally-activated shape memory effect. First of all, we verify for the first time that PLA electrospun fiber mats are able to present shape memory behavior at 60ºC, indicating that the electrospun

process does not affect the shape memory response own of PLA material. Moreover, all the plasticized electrospun samples (PLA-OLA) showed shape memory properties at 60ºC even if their recuperation starts at lower temperature. In fact, due to the addition of plasticizer the thermally-activated shape memory response can be studied at temperature close to the human body, such as 45ºC and 40ºC. The best formulation obtained to be used in this range is the PLA-OLA 80:20 showing excellent values of strain fixity ratio (higher than 95%) and strain recovery ratio of 100% in all the thermo-mechanical cycles at 45ºC with similar values at 40ºC. Thus, in view of these results, electrospun PLA-OLA 80:20 system can be described as a promising material to be used in potential shape memory biomedical applications with excellent R_f and R_r at temperature close to the physiological one.

5. Acknowledgements

Authors thank the Spanish Ministry of Economy, Industry and Competitiveness (MINEICO) (MAT2017-88123-P, POLYMAGIC: (PCIN-2017-036) cofinanced with FEDER funds. A.S. and L.P. acknowledge the "Juan de la Cierva" (FJCI-2015-24405) and "Ramon y Cajal" (RYC-2014-15595) contracts from MINEICO, respectively.

6. References

[1] T. Liu, T. Zhou, Y. Yao, F. Zhang, L. Liu, Y. Liu, J. Leng, Stimulus methods of multi-functional shape memory polymer nanocomposites: A review, Compos. Part A Appl. Sci. Manuf. 100 (2017) 20–30. doi:10.1016/j.compositesa.2017.04.022.

[2] M. Balk, M. Behl, C. Wischke, J. Zotzmann, A. Lendlein, Recent advances in degradable lactide-based shape-memory polymers, Adv. Drug Deliv. Rev. 107 (2016) 136–152. doi:10.1016/j.addr.2016.05.012.

[3] V. Sessini, J.M. Raquez, D. Lourdin, J.E. Maigret, J.M. Kenny, P. Dubois, L. Peponi, Humidity-Activated Shape Memory Effects on Thermoplastic Starch/EVA Blends and Their Compatibilized Nanocomposites, Macromol. Chem. Phys. 218 (2017) 1–12. doi:10.1002/macp.201700388.

[4] V. Sessini, J.M. Raquez, G. Lo Re, R. Mincheva, J.M. Kenny, P. Dubois, L. Peponi, Multiresponsive Shape Memory Blends and Nanocomposites Based on Starch, ACS Appl. Mater. Interfaces. 8 (2016) 19197–19201. doi:10.1021/acsami.6b06618.

[5] H. Jiang, S. Kelch, A. Lendlein, Polymers move in response to light, Adv. Mater. 18 (2006) 1471–1475. doi:10.1002/adma.200502266.

[6] F. Pilate, A. Toncheva, P. Dubois, J.M. Raquez, Shape-memory polymers for multiple applications in the materials world, Eur. Polym. J. 80 (2016) 268–294. doi:10.1016/j.eurpolymj.2016.05.004.

[7] L. Peponi, I. Navarro-Baena, J.M. Kenny, 7 - Shape memory polymers: properties, synthesis and applications, in: M.R. Aguilar, J.B.T.-S.P. and their A. San Román (Eds.), Woodhead Publishing, 2014: pp. 204–236. doi:https://doi.org/10.1533/9780857097026.1.204.

[8] J. Leng, X. Lan, Y. Liu, S. Du, Shape-memory polymers and their composites: Stimulus methods and applications, Prog. Mater. Sci. 56 (2011) 1077–1135. doi:10.1016/j.pmatsci.2011.03.001.

[9] J. Hu, Y. Zhu, H. Huang, J. Lu, Recent advances in shape-memory polymers: Structure, mechanism, functionality, modeling and applications, Prog. Polym. Sci. 37 (2012) 1720–1763. doi:10.1016/j.progpolymsci.2012.06.001.

[10] P. Sagitha, C.R. Reshmi, S.P. Sundaran, A. Sujith, Recent advances in post-modification strategies of polymeric electrospun membranes, Eur. Polym. J. 105 (2018) 227–249. doi:10.1016/j.eurpolymj.2018.05.033.

[11] C. Huang, N.L. Thomas, Fabricating porous poly(lactic acid) fibres via electrospinning, (2018). doi:10.1016/j.eurpolymj.2017.12.025.

[12] S. Agarwal, A. Greiner, J.H. Wendorff, Functional materials by electrospinning of polymers, Prog. Polym. Sci. 38 (2013) 963–991. doi:10.1016/j.progpolymsci.2013.02.001.

[13] Z.R. Ege, A. Akan, F.N. Oktar, C.C. Lin, B. Karademir, O. Gunduz, Encapsulation of indocyanine green in poly(lactic acid) nanofibers for using as a nanoprobe in biomedical diagnostics, Mater. Lett. 228 (2018) 148–151. doi:10.1016/j.matlet.2018.06.008.

[14] D. da Silva, M. Kaduri, M. Poley, O. Adir, N. Krinsky, J. Shainsky-Roitman, A. Schroeder, Biocompatibility, biodegradation and excretion of polylactic acid (PLA) in medical implants and theranostic systems, Chem. Eng. J. 340 (2018) 9–14. doi:10.1016/j.cej.2018.01.010.

[15] L. Peponi, V. Sessini, M.P. Arrieta, I. Navarro-Baena, A. Sonseca, F. Dominici, E.

Gimenez, L. Torre, A. Tercjak, D. López, J.M. Kenny, Thermally-activated shape memory effect on biodegradable nanocomposites based on PLA/PCL blend reinforced with hydroxyapatite, Polym. Degrad. Stab. 151 (2018) 36–51. doi:10.1016/j.polymdegradstab.2018.02.019.

[16] M.P. Arrieta, J. López, D. López, J.M. Kenny, L. Peponi, Development of flexible materials based on plasticized electrospun PLAâ€“PHB blends: Structural, thermal, mechanical and disintegration properties, (2015). doi:10.1016/j.eurpolymj.2015.10.036.

[17] M. Michalak, I. Krucińska, A smart textile fabric with two-way action, Text. Res. J. 88 (2018) 2044–2054. doi:10.1177/0040517517715086.

[18] B. Yan, S. Gu, Y. Zhang, Polylactide-based thermoplastic shape memory polymer nanocomposites, Eur. Polym. J. 49 (2013) 366–378. doi:10.1016/j.eurpolymj.2012.09.026.

[19] L. Peponi, I. Navarro-Baena, A. Sonseca, E. Gimenez, A. Marcos-Fernandez, J.M. Kenny, Synthesis and characterization of PCL-PLLA polyurethane with shape memory behavior, Eur. Polym. J. 49 (2013) 893–903. doi:10.1016/j.eurpolymj.2012.11.001.

[20] F. Khademeh Molavi, I. Ghasemi, M. Messori, M. Esfandeh, Nanocomposites based on poly(L-lactide)/poly(ε-caprolactone) blends with triple-shape memory behavior: Effect of the incorporation of graphene nanoplatelets (GNps), Compos. Sci. Technol. 151 (2017) 219–227. doi:10.1016/j.compscitech.2017.08.021.

[21] M. Behl, A. Lendlein, Shape-memory polymers, Mater. Today. 10 (2007) 20–28. doi:10.1016/S1369-7021(07)70047-0.

[22] Á. Sonseca, O. Menes, E. Giménez, A comparative study of the mechanical, shape-memory, and degradation properties of poly(lactic acid) nanofiber and cellulose nanocrystal reinforced poly(mannitol sebacate) nanocomposites, RSC Adv. 7 (2017) 21869–21882. doi:10.1039/C7RA01256J.

[23] V. Sessini, I. Navarro-Baena, M.P. Arrieta, F. Dominici, D. López, L. Torre, J.M. Kenny, P. Dubois, J.M. Raquez, L. Peponi, Effect of the addition of polyester-grafted-cellulose nanocrystals on the shape memory properties of biodegradable PLA/PCL nanocomposites, Polym. Degrad. Stab. 152 (2018) 126–138. doi:10.1016/j.polymdegradstab.2018.04.012.

[24] W. Koosomsuan, M. Yamaguchi, P. Phinyocheep, K. Sirisinha, High-Strain Shape Memory Behavior of PLA-PEG Multiblock Copolymers and Its Microstructural Origin,

J. Polym. Sci. Part B Polym. Phys. 57 (2019) 241–256. doi:10.1002/polb.24775.

[25] F.R. Lamastra, D. Puglia, M. Monti, A. Vella, L. Peponi, J.M. Kenny, F. Nanni, Poly(ε-caprolactone) reinforced with fibres of Poly(methyl methacrylate) loaded with multiwall carbon nanotubes or graphene nanoplatelets, Chem. Eng. J. 195–196 (2012) 140–148. doi:10.1016/j.cej.2012.04.078.

[26] M. Arrieta, A. Díez García, D. López, S. Fiori, L. Peponi, Antioxidant Bilayers Based on PHBV and Plasticized Electrospun PLA-PHB Fibers Encapsulating Catechin, Nanomaterials. 9 (2019) 346. doi:10.3390/nano9030346.

[27] X. Zhang, M.A. Geven, D.W. Grijpma, T. Peijs, J.E. Gautrot, Tunable and processable shape memory composites based on degradable polymers, Polymer (Guildf). 122 (2017) 323–331. doi:10.1016/j.polymer.2017.06.066.

[28] X. Luo, P.T. Mather, Preparation and Characterization of Shape Memory Elastomeric Composites, Macromolecules. 42 (2009) 7251–7253. doi:10.1021/ma9015888.

[29] M.P. Arrieta, J. López, D. López, J.M. Kenny, L. Peponi, Biodegradable electrospun bionanocomposite fibers based on plasticized PLA–PHB blends reinforced with cellulose nanocrystals, Ind. Crops Prod. 93 (2016) 290–301. doi:10.1016/j.indcrop.2015.12.058.

[30] N. Burgos, D. Tolaguera, S. Fiori, A. Jiménez, Synthesis and Characterization of Lactic Acid Oligomers: Evaluation of Performance as Poly(Lactic Acid) Plasticizers, J. Polym. Environ. 22 (2014) 227–235. doi:10.1007/s10924-013-0628-5.

[31] M.P. Arrieta, M.D.M. Castro-López, E. Rayón, L.F. Barral-Losada, J.M. López-Vilariño, J. López, M.V. González-Rodríguez, Plasticized poly(lactic acid)-poly(hydroxybutyrate) (PLA-PHB) blends incorporated with catechin intended for active food-packaging applications, J. Agric. Food Chem. 62 (2014) 10170–10180. doi:10.1021/jf5029812.

[32] C. Guo, L. Zhou, J. Lv, Effects of expandable graphite and modified ammonium polyphosphate on the flame-retardant and mechanical properties of wood flour-polypropylene composites, Polym. Polym. Compos. 21 (2013) 449–456. doi:10.1002/app.

[33] S. Jacobsen, H.G. Fritz, Plasticizing polylactide?the effect of different plasticizers on the mechanical properties, Polym. Eng. Sci. 39 (1999) 1303–1310. doi:10.1002/pen.11517.

[34] N. Ljungberg, B. Wesslén, Preparation and properties of plasticized poly(lactic acid) films, Biomacromolecules. 6 (2005) 1789–1796. doi:10.1021/bm050098f.

[35] O. Martin, L. Averous, Plasticization and properties of biodegradable multiphase systems polymer, Polymer (Guildf). 42 (2001) 6209–6219.

[36] A. Mujica-Garcia, I. Navarro-Baena, J.M. Kenny, L. Peponi, Influence of the Processing Parameters on the Electrospinning of Biopolymeric Fibers, J. Renew. Mater. 2 (2014) 23–34. doi:10.7569/JRM.2013.634130.

[37] S. Carrasco-Hernandez, J. Gutierrez, L. Peponi, A. Tercjak, Optimization of the electrospinning processing-window to fabricate nanostructured PE-b-PEO and hybrid PE-b-PEO/EBBA fibers, Polym. Eng. Sci. 57 (2017) 1157–1167. doi:10.1002/pen.24492.

[38] D. Garlotta, A Literature Review of Poly (Lactic Acid), J. Polym. Environ. 9 (2002) 63–84. doi:10.1023/A:1020200822435.

[39] A. Ni Annaidh, K. Bruyere, M. Destrade, M.D. Gilchrist, M. Ottenio, Characterization of the anisotropic mechanical properties of excised human skin., J. Mech. Behav. Biomed. Mater. 5 (2012) 139–148. doi:10.1016/j.jmbbm.2011.08.016.

[40] S. Pal, Design of artificial human joints & organs, Des. Artif. Hum. Joints Organs. 9781461462 (2014) 1–419. doi:10.1007/978-1-4614-6255-2.

[41] G.A. HOLZAPFEL, Biomechanics of Soft Tissue, Handb. Mater. Behav. Model. (2001) 1057–1071. doi:10.1016/B978-012443341-0/50107-1.

[42] Y. Liu, S. Wang, R. Zhang, Composite poly(lactic acid)/chitosan nanofibrous scaffolds for cardiac tissue engineering, Int. J. Biol. Macromol. 103 (2017) 1130–1137. doi:10.1016/j.ijbiomac.2017.05.101.

[43] X. Zhang, X. Lu, Z. Wang, J. Wang, Z. Sun, Biodegradable shape memory nanocomposites with thermal and magnetic field responsiveness, J. Biomater. Sci. Polym. Ed. 24 (2013) 1057–1070. doi:10.1080/09205063.2012.735098.